

Nitrogen laser with a pulse repetition rate of 11 kHz and a beam divergence of 0.5 mrad

V.V. Atezhev, S.K. Vartapetov, A.K. Zhigalkin, K.E. Lapshin, A.Z. Obidin

Abstract. A repetitively pulsed high-frequency UV nitrogen laser based on magnetic pulse compression (MPC) circuit is developed. The special characteristics of laser operation at pulse repetition rates up to 11 kHz are studied. Lasing with an average power of 1.4 W for a beam divergence of less than 0.5 mrad is obtained.

Keywords: nitrogen laser, pulse discharge, magnetic pulse compression, high pulse repetition rate.

1. Introduction

The demand for UV range lasers with an average radiation power of 1–10 W has been increasing constantly for solving applied and fundamental research problems. The UV radiation sources are usually excimer lasers or solid-state lasers with frequency conversion. However, an electric-discharge laser based on nitrogen molecules (N_2 laser) generating short pulses ($\tau < 10$ ns) at a wavelength $\lambda = 337$ nm can serve as an alternative to these lasers in the output power range mentioned above. Due to a relatively simple and reliable design N_2 lasers may be considerably cheaper than the existing lasers operating in the UV range. Nitrogen lasers are used for preparing and retouching of photomasks, micromarking, dye laser pumping, etc. Such lasers are especially expedient when UV radiation is used for ecologically clean production and for medical purposes where stringent requirements are imposed on the safety and cleanliness of the surrounding medium.

The possibility of generating single pulses in nitrogen lasers with an energy of several tens of millijoules [1], attaining pulse repetition rates up to several kilohertz and the average power of up to 20 W [2–4] was demonstrated in several works. The use of nitrogen lasers is frequently impaired due to a low average power and a high beam divergence. Increasing the radiation pulse energy of nitrogen lasers is not effective since the low efficiency of such lasers leads to a sharp increase in their size and to complications in designing low-inductive discharge circuits.

V.V. Atezhev, S.K. Vartapetov, A.K. Zhigalkin, K.E. Lapshin, A.Z. Obidin Physics Instrumentation Center, A.M. Prokhorov General Physics Institute, Russian Academy of Sciences, 142190 Troitsk, Moscow region, Russia; e-mail: kos@pic.troitsk.ru; Tel.: (095) 334 02 12; Fax: (095) 334 02 16; web-site: <http://www.pic.troitsk.ru>

Received 1 April 2004; revision received 21 June 2004

Kvantovaya Elektronika 34 (9) 790–794 (2004)

Translated by Ram Wadhwa

Besides, an increase in the size of the discharge system usually leads to an increase in the beam divergence.

From the point of view of increasing the average radiation power of nitrogen lasers, a more rational approach is to increase the laser pulse repetition rate. It is well known that this increase is attained by increasing the gas circulation rate in the discharge gap, decreasing the size of the discharge zone in the direction of gas flow, ensuring a high uniformity of volume discharge of the pump, lowering the specific energy contribution to the discharge [5], as well as by damping the acoustic vibrations caused in the pump volume by the previous discharge [6]. However, not all the problems connected with the operation of pulsed gas (nitrogen, excimer, CO_2) lasers have been solved for high pulse repetition rates.

The aim of this study was to create a UV nitrogen laser with a small beam divergence, a pulse repetition rate $f \geq 10$ kHz, and the average radiation power $P > 1$ W, as well as to study the output parameters and operating conditions in this frequency range.

2. Laser design

The gas-discharge chamber is constructed according to the conventional design of a TEA laser with a closed gas-circulation loop and is placed in a cylindrical casing made of an aluminium alloy with an inner diameter 240 mm and length 180 mm (Fig. 1). High-voltage cathode (1) and grounded anode (2) have an easy-to-prepare cylindrical working surface of radius 1.5 mm, width 3 mm and length 120 mm. The electrodes are mounted on an easily detachable cover made of an insulating material and are separated by a discharge gap $d = 8$ mm. To reduce the electric field strength in the region of the gas outlet from the discharge gap, the return current lead connecting the anode with outer peaking capacitors (3) was situated only in the confusor part of the circulation circuit. To reduce the kinetic energy losses in the gas flow at the outlet from the discharge gap, the diffuser has a flare angle of 15° at a length of 120 mm, and gas flow guides (7) are installed at the places of turning of the flow [7].

Pulsed corona discharge from the knife edge of preioniser (4) short-circuited with the high-voltage cathode served as the source of preionisation. The knife edge is located in the plane of the insulating wall surface of the gas-circulation loop and hence does not disturb the gas flow. A preioniser of such a design consumes a fraction of one percent of the energy supplied to the pump discharge and does not create any shock waves that deteriorate the uniformity of the main

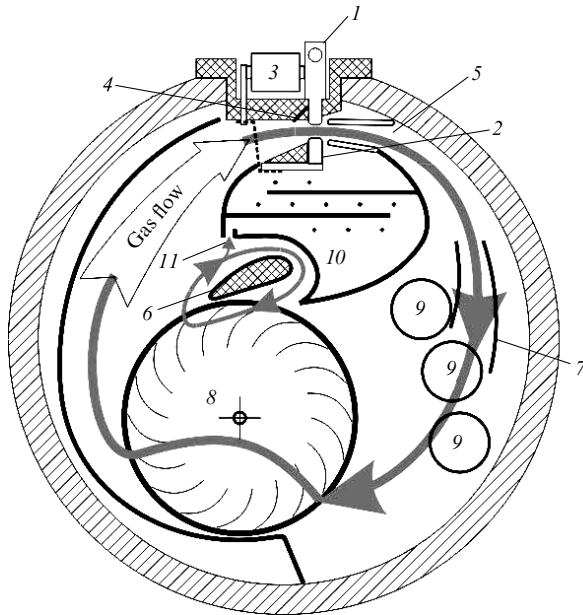


Figure 1. Cross section of a gas-discharge chamber: (1) high-voltage cathode; (2) grounded anode; (3) peaking capacitor; (4) knife-edge preioniser; (5) diffuser; (6) vortex-former of the tangential fan; (7) flow-forming guides; (8) impeller of the tangential fan; (9) water-cooled radiators; (10) electrostatic filter; (11) gas inlet to the electrostatic filter.

discharge. Its electrodes practically do not disperse and hence do not contaminate the working mixture.

Gas circulation is carried out by a tangential fan of diameter 110 mm. The aerodynamic contour of pumping was designed by the authors in collaboration with a branch of the Central Aerohydrodynamics Institute [8]. In contrast to the ordinary pump scheme, vortex-former (6) is included in the outlet branch pipe in the gas circulation circuit. Such a fan has the relative aerodynamic pressure up to three times higher than a common fan at small flow. Fan (8) was rotated by an asynchronous electric motor through a sealing magnetic clutch, and the rotational frequency can be varied gradually. Tubular lamellar-ribbed water-cooled radiators (9) with an overall area of 0.36 m^2 for heat removal from the gas were installed in the dilated part of the circuit.

To clean the gas from the dust formed as a result of electrode erosion, electrostatic filter (10) was installed in the central region of the gas circulation circuit. Gas inlet (11) to the filter is located in the outlet branch pipe of the fan, namely, the highest-pressure zone in the circuit.

It is well known that an effective excitation of the nitrogen laser requires the most powerful and rapid pumping of the active medium, which is carried out near the peak U_m of the discharge voltage [6]. In this case, a significant part of the stored electric energy is supplied to the active zone for an elevated reduced field voltage $E/p > 100 \text{ V cm}^{-1} \text{ Torr}^{-1}$ required for an effective excitation of the upper laser level $C^3\Pi_u$. In order to realise such excitation conditions for a high pulse repetition rate, we used a high-voltage generator with a thyratron switched MPC circuit described in [9].

In this work, we have studied several versions of high-voltage MPC-circuit-based generator. The number of compression stages varied from one to four. Figure 2 shows the circuit of a high-voltage generator with three compression stages. Our investigations showed that this circuit was the

most effective one. Capacitors $C_1 - C_6$ had the same capacitance equal to 1 nF. The capacitance C_p of the peaking capacitor was 0.57 nF. The inductances of the magnetic compression stages indicated in the circuit correspond to the saturated state of the cores. Each nonlinear inductive element is a series-parallel connection of several inductances wound on ferrite rings. All elements of the pump generator except the peaking capacitor and thyratron are immersed in transformer oil which is cooled. Such a construction is compact and ensures the required thermal regime for the ferrite cores. Magnetisation reversal of all the cores of compression stages is carried out by the current used to charge the reservoir capacitor C_2 , passing from the high-voltage pulsed power supply successively through all the coils of compression stages.

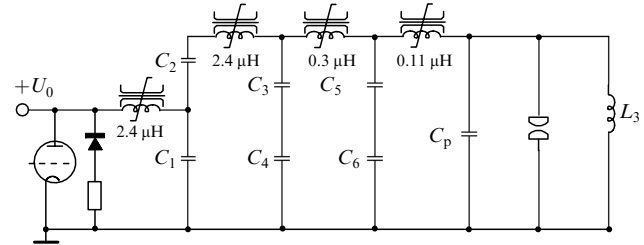


Figure 2. Electrical circuit of a high-voltage N_2 laser pump generator with three compression stages; $C_{1-6} = 1 \text{ nF}$, $C_p = 0.57 \text{ nF}$.

Table 1 shows the parameters of four investigated pump oscillator circuits, obtained for a supply voltage of 12 kV, pump pulse repetition rate $f = 2 \text{ kHz}$, and nitrogen pressure of 170 mbar in the discharge chamber of the laser. The generator efficiency was determined as the ratio of the energy accumulated in the capacitor C_p at the instant of breakdown of the discharge gap to the energy stored in the capacitors $C_1 + C_2$.

It follows from the experimental data presented in Table 1 that the efficiency of the laser depends on the power released at the initial stage of the discharge ($\sim U_m^2 L^{-1/2}$) [3]. The efficiency is higher for higher voltage U_m across the capacitor C_p , and lower inductance L (saturated inductance of the last compression stage) through which the capacitor is charged. The maximum total efficiency (0.1%) of the laser is attained in a generator circuit with three magnetic compression stages. One can see from the data presented in Table 1 that even a relatively

Table 1.

Parameter	Pump generator circuits with different numbers of compression stage			
	1	2	3	4
Thyratron current duration/ns	70	150	150	450
Thyratron current amplitude/A	500	250	250	80
Voltage amplitude across the peaking capacitor/kV	13.6	13.6	13.7	13.1
Rise time of voltage across the peaking capacitor/ns	24	24	14	14
Efficiency of MPC generator (%)	36	36	37	34
Lasing energy/ μJ	105	111	139	126
Laser efficiency (%)	0.075	0.08	0.1	0.09

small compression of the voltage front attained in the third link leads to a considerable increase in the pump efficiency. A four-compression-stage circuit considerably lowers the thyratron current and the starting losses, and the total efficiency of the laser is also slightly lower. Thus, a four-stage generator circuit is preferable only for increasing the lifetime of the thyratron.

An unstable resonator whose optical diagram is shown in Fig. 3 was used for obtaining radiation with a small beam divergence. A peculiarity in the design of this resonator is that the output mirror is a fragment of a spherical surface with a characteristic size ~ 1.5 mm, displaced from the resonator axis towards the edge of the discharge gap. For such an arrangement of the output mirror of the resonator, the output radiation beam has a quite uniform intensity distribution over the cross section in which there is no dark spot at the centre.

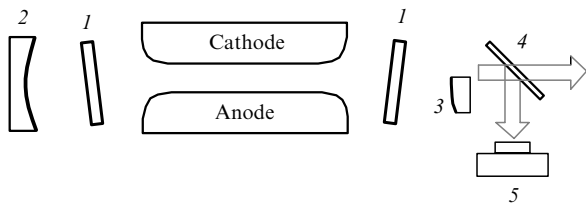


Figure 3. Scheme of the N_2 -laser resonator: (1) front and rear sealing quartz windows; (2) concave mirror; (3) convex mirror at the radiation output; (4) beam-splitting plate; (5) IMO-2 power meter.

3. Experimental results

The mean flow velocity in the discharge gap was measured by the MMN-2400-1.0 micromanometer in the laser gas-discharge chamber filled with atmospheric air. The mean velocity v of the working gas (nitrogen under a pressure of 200–300 mbar), recalculated by using Reynolds similitude criterion for the maximum rotational velocity 5800 rpm of the fan impeller, was found to be more than 55 m s^{-1} .

The discharge cross section was $1.6 \times 8 \text{ mm}$. As the pulse repetition rate increased to a certain limiting value f_{\lim} , the mean output power was found to increase. Upon a further increase in f ($f > f_{\lim}$), a sharp decrease in the output

power was observed due to the emergence of the competing electrical breakdown which shunted the pump discharge. The quantity f_{\lim} increased linearly with the rotational frequency of the fan impeller and attained a value of 6.1 kHz for the maximal rotational frequency. The breakdown emerges between the lateral surfaces of the laser electrodes on the side of the gas flow outlet from the discharge gap at a distance $d \leq 5 \text{ mm}$ from the pump discharge. At this frequency, the flow carries away the main part of the gas processed during the preceding pump pulse to a distance $\Delta = v/f_{\lim} > 9 \text{ mm}$, which is considerably larger than 5 mm and cannot be the main reason for the emergence of the competing breakdown.

The constraints imposed on f_{\lim} may be due to several factors. In the pulsed TEA lasers, it is quite difficult to ensure the smooth linking of the electrode profile with the walls of the gas channels without distorting the electric field that forms the pump discharge. This may lead to a return flow behind the electrodes, whose magnitude increases with the gas velocity [11].

In addition, the flow velocity near the channel walls is considerably lower than the main flow velocity. The products of the action of a high-current discharge on the gaseous medium and the material of the electrodes are concentrated in layers adjoining the electrodes. In all probability, the competing breakdown is initiated by highly ionised discharge products remaining in the electrode regions after the passage of the previous pulse (Fig. 4a). Indeed, the electron concentration in nitrogen after the passage of the exciting pulse can be determined by using formula (1) from [10]:

$$n_e = \frac{n_0}{1 + \beta n_0 t} \approx \frac{1}{\beta t},$$

where β is the coefficient of dissociative electron-ion recombination. For nitrogen, $\beta \approx 2 \times 10^{-7} \text{ cm}^3 \text{ s}^{-1}$ and $n_0 \sim 10^{14} \text{ cm}^{-3}$ is the concentration of the plasma formed as a result of ionisation-induced electron multiplication in the discharge gap. For the interval $t = f^{-1} < 1.7 \times 10^{-4} \text{ s}$ ($f > 6 \text{ kHz}$) between pulses, we find that $n_e > 10^{11} \text{ cm}^{-3}$. This means that at the time of arrival of the next pulse, the products of the previous discharge are preserved in the form of a plasma with an electron concentration much

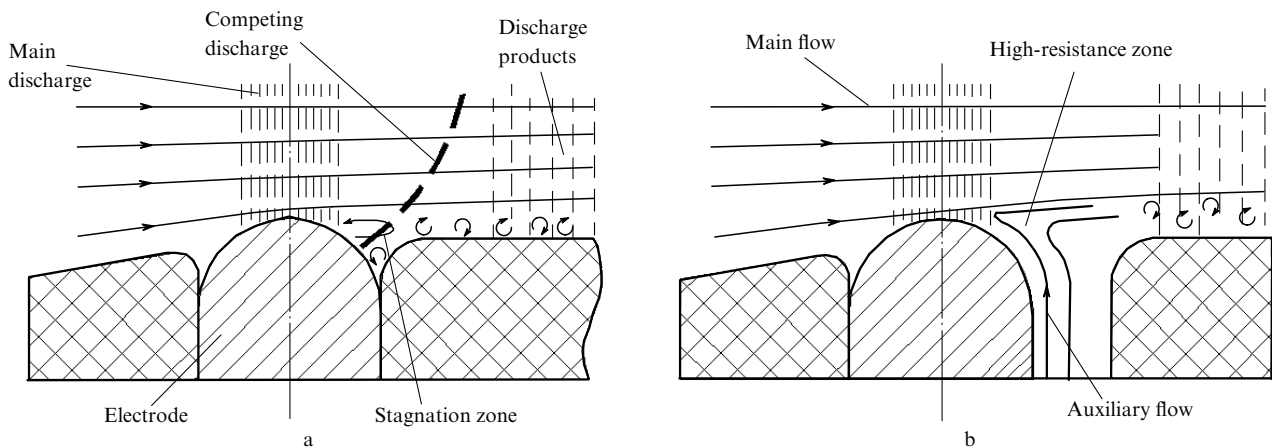


Figure 4. Cross section of the electrode region: (a) formation of competing discharge and (b) substitution of neutral gas for ionised gas by using an auxiliary flow.

higher than the initial value ($n_e < 10^8 \text{ cm}^{-3}$) [12] resulting from the preionisation of the discharge gap.

It is well known [13] that, as a result of polarisation, plasma screens the electric field in the volume occupied by it and enhances the field outside this volume. This process has a characteristic time $\tau = (4\pi\mu en_e)^{-1}$, where μ and e are the electron mobility and charge respectively. For the condition of our experiments (nitrogen pressure $p \approx 200 \text{ mbar}$, $\mu \approx 2.2 \times 10^3 \text{ cm}^2 \text{ V}^{-1} \text{ s}^{-1}$ [14]), $\tau \approx 2.5 \times 10^{-9} \text{ s}$, which is much shorter than the duration of the voltage front across the discharge gap (see Table 1). Hence the effect of highly ionised plasma on the breakdown conditions in the discharge is analogous to the effect of a conductor having the shape of the volume occupied by the plasma. Thus plasma can distort the field formed by the electrode and initiate a competing breakdown.

In order to reduce the harmful effects of the above-mentioned factors, the gas circulation circuit was modified by introducing an additional channel of width about 1.5 mm along the entire lateral surface of each electrode on the side of the gas outlet from the discharge gap (Fig. 4b). After passing through a cooling system and an electrostatic cleaning device, the gas was supplied to the discharge zone through these channels [15]. No additional circulation facilities were required for this purpose since the inlet and outlet of the channels were matched respectively with the high- and low-pressure zones of the gas-circulation circuit. This made it possible to increase the electric strength of the gas in the regions near the electrodes and hence increase the pulse repetition rate f_{lim} to 11 kHz.

In the course of the experiment, the composition and pressure of the gas mixture were optimised in accordance with the maximum average radiation power at every 500 Hz (Fig. 5). The output power of the laser for $f \leq 3 \text{ kHz}$ was the highest in a helium-free mixture under a pressure of 200 mbar of pure nitrogen. Further increase in the value of f while preserving the pulse energy was attained in $\text{N}_2 - \text{He}$ by adding helium to the working mixture. For $f = 11 \text{ kHz}$, the optimal mixture contained nitrogen under a partial pressure of 140 mbar (for a total pressure 560 mbar of the working mixture). An increase in the thermal conductivity of the working gas (the thermal conductivity of helium is six times the thermal conductivity of nitrogen) leads to higher frequencies at which the critical growth of inhomogeneities

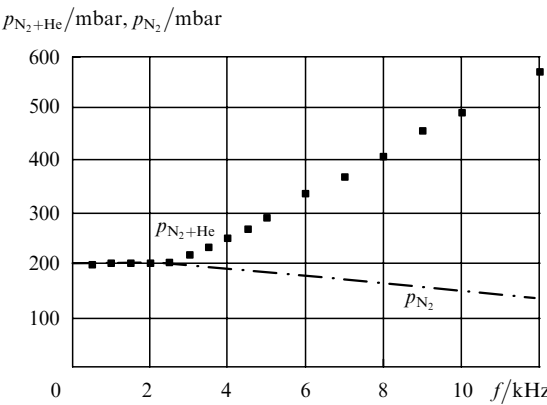


Figure 5. Dependences of the optimal pressure p_{N_2} of nitrogen and pressure $p_{\text{N}_2+\text{He}}$ of the nitrogen-helium mixture on the pulse repetition rate f .

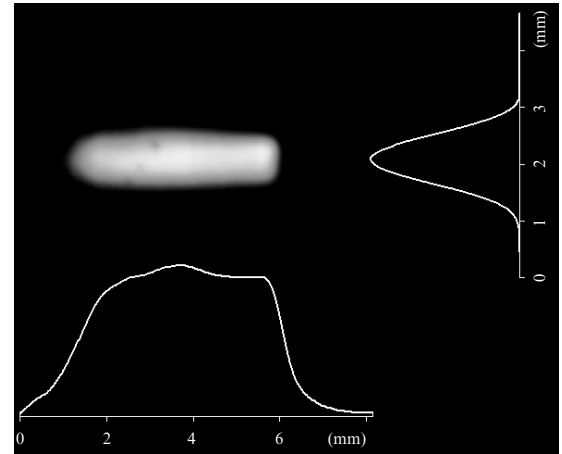


Figure 6. Intensity distribution in the output laser beam measured at a distance of 30 cm from the output aperture.

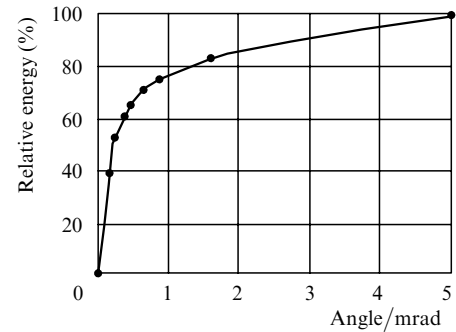


Figure 7. Results of divergence measurement by the focal spot method.

begins in the pumping discharge volume. A stable laser operation with an average radiation power of 1.4 W is observed in the optimised working gas mixture at the highest pulse repetition rate.

The laser beam had a rectangular cross section of size $1.5 \times 6 \text{ mm}$. For a separation of 230 mm between the mirrors, the highest energy was obtained in an unstable telescopic resonator with a magnification $M = 3.8$ (the results for $M = 2.9, 3.8, 5.6$ and 7.5 were compared). Fig. 6 shows the intensity distribution in the output laser beam, while Fig. 7 shows the results of measurement of divergence by the focal spot method. The angular divergence of the output radiation, measured at 50 % of the total energy, was found to be 0.4 mrad. The laser pulse shape is shown in Fig. 8. The pulse FWHM was 3.5 ns.

Prolonged operation of the lasers showed that the average radiation power of the laser decreases by about 1 % per every million pulses (without the replacement of the gas mixture). For a partial replacement of the gas mixture through the introduction of small portions (15 mbar), the laser attained steady-state generation after 3×10^6 pulses and worked continuously at a constant output power throughout the day. The use of an electrostatic filter for purification of the working gas from the electrode sputtering products ensured an operating life of more than 10^{10} pulses for the output windows.

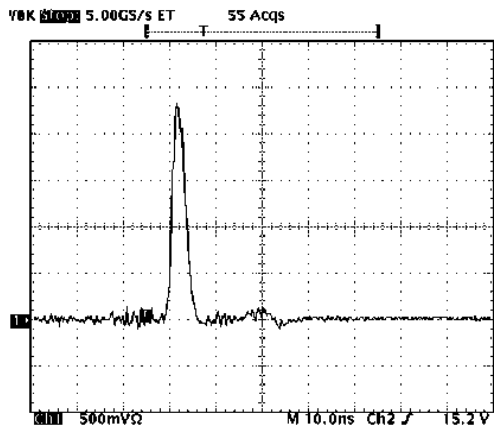


Figure 8. Laser pulse shape.

4. Conclusions

We have developed a nitrogen laser with an average output power of 1.4 W and a beam divergence of less than 0.5 mrad. It is found that when a magnetic pulse compression oscillator is used, the three-stage scheme is the most effective for pumping a repetitively pulsed N₂ laser.

It is shown that the highly ionised plasma left after the previous pump discharge, which is situated near the discharge gap due to a poor streamlining of the electrode contour and provokes a competing breakdown, prevents an increase in the laser pulse repetition rate. The expulsion of the products of the previous discharge by a neutral gas supplied through additional gas channels increases the electric strength of the gas in the electrode regions and raises the limiting frequency f_{lim} to 11 kHz. Moreover, a stable operation of the laser at high repetition rates requires an increase in the thermal conductivity of the working gas through the addition of helium.

The results presented in this publication were obtained in the course of research aimed at creating a UV laser for titling of cinema films, carried out by the authors at the behest and with the support of Cinema magnetique communication, France.

References

- doi> 1. Armandilo E., Kearsley A.J. *Appl. Phys. Lett.*, **41** (7), 611 (1982).
2. Papakin V.F., Sonin A.Yu. *Kvantovaya Elektron.*, **5**, 1580 (1978) [*Sov. J. Quantum Electron.*, **8**, 901 (1978)].
3. Goldort V.G., Ischenko V.N., Kochubei S.A. *Proc. SPIE Int. Soc. Opt. Eng.*, **3574**, 649 (1998).
4. Kozlov B. *Proc. SPIE Int. Soc. Opt. Eng.*, **3574**, 643 (1998).
5. Dzakowic G.S., Wutzke S.A. *J. Appl. Phys.*, **41** (11), 5061 (1979).
- doi> 6. Borisov V.M., Borisov A.V., Bragin I.E., Vinokhodov A.Yu., *Kvantovaya Elektron.*, **22**, 446 (1995) [*Quantum Electron.*, **25**, 421 (1995)].
7. Ide'chik I.E. *Spravochnik po gidravlicheskim sопротивлениям* (Handbook on Hydraulic Resistance) (Moscow: Mashinostroenie, 1975).
8. Korovkin A.G., Klimova T.A., Feofilaktov A.N. *Promышленная Aerodinamika* (Industrial Aerodynamics) (Moscow: Mashinostroenie, 1991).
9. Ageev V.P., Atezhev V.V., Bukreev V.S., Vartapetov S.K., et al. *Zh. Tekh. Fiz.*, **56**, 1387 (1981).
10. Soloukhin R.I., Yakobi Yu.A., Vyazovich E.I., Vagin S.P. *Inzh. Fiz. Zh.*, **36**, 62 (1979).
11. Krasnov N.F., Danilov A.N., Zakharchenko V.F., Koshevoi V.N. *Osnovy prikladnoi aerogazodinamiki* (Fundamentals of Applied Aerogasdynamics) (Moscow: Vysshaya Shkola, 1991) Vol. 2.
12. Korolev Yu.D., Mesyats G.A. *Fizika impul'snogo proboya gazov* (Physics of Pulsed Breakdown of Gases) (Moscow: Nauka, 1991).
13. Raizer Yu.P. *Gas Discharge Physics* (Berlin: Springer-Verlag, 1991; Moscow: Nauka, 1987).
14. Mac-Daniel I. *Protsessy stolknovenii v ionizovannykh gazakh* (Collision Processes in Ionised Gases) (Russian translation) (Moscow: Mir, 1962).
15. Atezhev V.V. Russia Patent No. 2132104S1 (1997).